THE JOURNAL OF BIOLOGICAL CHEMISTRY
Vol. 278, No. 18, Issue of May 2, pp. 16271–16279, 2003

Printed in U.S.A.

Declusterization of $GABA_A$ Receptors Affects the Kinetic Properties of GABAergic Currents in Cultured Hippocampal Neurons*

Received for publication, December 23, 2002, and in revised form, February 24, 2003
Published, JBC Papers in Press, February 24, 2003, DOI 10.1074/jbc.M213081200

Enrica Maria Petrini‡, Paola Zacchi‡, Andrea Barberis‡§, Jerzy W. Mozrzymas¶‖, and Enrico Cherubini‡**

From the ‡Neuroscience Programme and Istituto Nazionale Fisica della Materia Unit, International School for Advanced Studies, Via Beirut 2-4, Trieste 34014, Italy and the ¶Department of Biophysics, Wroclaw Medical University, ul. Chalubinskiego 10, Wroclaw 50-368, Poland

Speed and reliability of synaptic transmission are essential for information coding in neuronal networks and require the presence of clustered neurotransmitter receptors at the plasma membrane in precise apposition to presynaptic terminals. Receptor clusterization is the result of highly regulated processes involving functional and structural proteins. Among the structural elements, microtubules are known to play a crucial role in anchoring of γ-aminobutyric acid, type A ($GABA_A$) receptors. Here we show that microtubule depolymerization with nocodazole induces the declusterization of $GABA_A$ receptors and modifies the kinetic properties of GABAergic currents in cultured hippocampal neurons. In particular, this drug, applied either in the bath or via the patch pipette, induced the acceleration of the onset kinetics of miniature inhibitory postsynaptic currents (mIPSCs) without significantly affecting their frequency, thus suggesting a main postsynaptic site of action. After nocodazole treatment, current responses to ultrafast applications of GABA exhibited a faster rise time and an accelerated onset of desensitization. A quantitative analysis of GABA-evoked currents and model simulations suggest that declusterization affects the gating properties of $GABA_A$ receptors. In particular, a faster entry into the desensitized state of declustered $GABA_A$ receptors may account for the changes in the kinetic properties of mIPSCs after nocodazole treatment. Hence it appears that the clustered condition of $GABA_A$ receptors contributes in shaping GABAergic currents.

Efficient GABAergic[1] synaptic transmission requires the presence of clustered postsynaptic $GABA_A$ receptors localized in precise apposition to presynaptic releasing sites. To form and maintain postsynaptic clusters, neurons must possess the ability to appropriately sort, target, cluster, recycle, and degrade $GABA_A$ receptors (1). All these processes are highly regulated and have been shown to rely on the presence of the intact cytoskeleton and on the interplay of functional proteins and intracellular factors (2, 3).

Among the proteins involved in delivering $GABA_A$ receptors to the membrane, $GABA_A$ receptor-associated protein (4) is thought to be crucial. In fact, not only does it show tubulin-binding activity (5) and interaction with the γ_2 subunit of $GABA_A$ receptors (4), but it also binds *N*-ethylmalemide sensitive factor, a protein that plays an essential role in intracellular membrane trafficking (6). The possible role of $GABA_A$ receptor-associated protein in $GABA_A$ receptors trafficking is strengthened by its sequence and structural similarities with mammals and yeast proteins involved in membrane dynamics and vesicular transport (7–10), suggesting that this protein could be specialized to recruit $GABA_A$ receptors into budding vesicles targeted to the postsynaptic membrane (3).

After the insertion into the plasma membrane, $GABA_A$ receptors may undergo clusterization. One of the major candidate molecules for synaptic $GABA_A$ receptor clustering is gephyrin (11–14), a tubulin-binding protein that has been shown to co-localize with $GABA_A$ receptors at postsynaptic sites (15). However, additional proteins must be involved in the clustering process (3), because biochemical approaches failed to show a direct interaction between gephyrin and $GABA_A$ receptors (16).

An increasing body of evidence indicates that the cytoskeleton is essential for clustering $GABA_A$ receptors (4, 17–20). The cytoskeleton is formed by a complex meshwork of microtubules, actin microfilaments, intermediate filaments, and many associated proteins. The state of polymerization of microtubules appears to contribute in modulating the activity of $GABA_A$ receptors (17–19). The disruption of microtubules with colchicine, vinblastine, and nocodazole has been shown to block muscimol-stimulated $^{36}Cl^-$ uptake into cortical microsacs and to inhibit GABA-mediated currents in *Xenopus laevis* oocytes expressing $GABA_A$ receptor subunits (17). Moreover, in cultured hippocampal neurons nocodazole treatment induced a rundown of muscimol-induced currents (18). Despite the efforts to clarify the cellular and molecular mechanisms regulating cytoskeleton-receptor interactions, this topic is still a matter of debate. In particular, it is unknown whether receptor clusterization may interfere with the gating properties of $GABA_A$ receptors.

In this study we induced the depolymerization of microtubules with nocodazole to alter the organization of $GABA_A$ receptor clusters in cultured hippocampal neurons. We found that declusterization of $GABA_A$ receptors was associated with an acceleration of the rise time of mIPSCs. Moreover, in diffuse $GABA_A$ receptors, current responses to ultrafast applications of GABA showed a faster onset and an accelerated desensitization. Model simulations suggested that the increased rate of

* This work was supported in part by the Ministero dell'Istruzione, dell'Universita' e della Ricerca (Grant COFI 2001 to E. C.). The costs of publication of this article were defrayed in part by the payment of page charges. This article must therefore be hereby marked "*advertisement*" in accordance with 18 U.S.C. Section 1734 solely to indicate this fact.

§ Present address: Dept. of Pharmacology and Toxicology, University of Zürich, Winterturerstrasse 190, Zürich CH-8057, Switzerland.

‖ Supported by the Polish Committee for Scientific Research (Grant 6P04A-001-19).

** To whom correspondence should be addressed. Tel.: 39-040-378-7223; Fax: 39-040-378-7528; E-mail: cher@sissa.it.

[1] The abbreviations used are: GABAergic, GABA-mediated; $GABA_A$, γ-aminobutyric acid, type A; mIPSC, miniature inhibitory postsynaptic current.

entry into the desensitized state might account for the accelerated onset kinetics of GABAergic currents.

EXPERIMENTAL PROCEDURES

Cell Culture—Primary cell cultures were prepared as previously described (21). Briefly, 2- to 4-day-old (P2–P4) Wistar rats were decapitated after being anesthetized with an intraperitoneal injection of urethane (2 mg/kg). This procedure is in accordance with the regulation of the Italian Animal Welfare Act and was approved by the local veterinary service authority. Hippocampus were dissected free, sliced, and digested with trypsin, mechanically triturated, centrifuged twice at $40 \times g$, plated in Petri dishes, and cultured for up to 14 days. Experiments were performed on cells cultured for at least 7 days.

Nocodazole Treatment—Nocodazole (purchased from Sigma, Milano, Italy) was used to disrupt microtubules. It was applied at the concentration of 10 μg/ml (22) from a 100% Me_2SO stock solution. The final concentration of Me_2SO in the working solutions was 0.1% (v/v). Nocodazole was applied in two different ways: in the culture medium (bath treatment) and via the patch pipette (intrapipette application). Bath treatment consisted of adding the drug to the neuronal culture medium and incubating the cells at 37 °C for 2 h. Because the effects of nocodazole are reversible, in electrophysiological experiments the drug was added to the extracellular and intracellular solutions (10 μg/ml). To verify whether Me_2SO itself could affect synaptic transmission, some electrophysiological experiments ($n = 12$) were performed also on cells incubated with Me_2SO alone in the culture medium at 37 °C for 2 h. Me_2SO 0.1% (v/v) did not produce any change in the kinetic properties of mIPSCs. Intrapipette application consisted of adding nocodazole to the intracellular solution to apply the drug only to the recorded cell via the patch pipette (18, 23).

Immunofluorescence Staining—Immunocytochemistry for the γ_2 subunit of the GABA$_A$ receptor was performed to analyze the organization of GABA$_A$ receptors on the neuronal membrane both before and after bath treatment with nocodazole as described above. After fixation with 4% paraformaldehyde, hippocampal neurons seeded on coverslips were washed with phosphate-buffered saline, blocked with 5% normal serum, and incubated with an affinity-purified polyclonal antibody raised against the amino-terminal region of the γ_2 subunit (γ_2[1–33]R13/7, kindly provided by W. Sieghart, University of Wien, Austria). The resulting immune complex was visualized with fluorescein isothiocyanate-labeled goat anti-rabbit IgG (Sigma, Milano, Italy). Note that the receptors labeled were only those expressed on the cell surface, because the incubation with the anti-GABA$_A$ receptor γ_2 subunit antibody was performed on non-permeabilized cells. To evaluate the disruptive effect of nocodazole on the microtubular network, the same hippocampal neurons were then used for a second immunocytochemical experiment using an antibody against tubulin. Cells were then permeabilized with 0.1% Nonidet P-40, washed with phosphate-buffered saline, blocked with 5% normal serum, and incubated with a rat monoclonal anti-tubulin antibody. The resulting immune complexes were visualized with tetramethyl rhodamine isothiocyanate-labeled rabbit anti-rat IgG (Sigma, Milano, Italy). Neurons were imaged with the Olympus (BX51WI) confocal system by using sequential dual-channel recording of double-labeled cells.

Electrophysiological Recordings—Currents were recorded in the whole-cell and outside-out configurations of the patch-clamp technique using an EPC-7 amplifier (List Medical, Darmstadt, Germany). In the case of whole-cell recordings, the stability of the patch was checked by repetitively monitoring the input and series resistance during the experiments. Cells exhibiting changed values were excluded from the analysis. The series resistance (R_s) was in the range of 4–8 MΩ. Both mIPSCs and GABA-evoked currents were recorded at a holding potential of −70 mV. The intrapipette solution contained (in millimolar): CsCl 137, $CaCl_2$ 1, $MgCl_2$ 2, 1,2-bis(2-aminophenoxy)ethane-*N*,*N*,*N*9-tetraacetic acid 11, ATP 2, and HEPES 10, pH 7.2, with CsOH. The composition of the external solution was (in millimolar): NaCl 137, KCl 5, $CaCl_2$ 2, $MgCl_2$ 1, glucose 20, and HEPES 10, pH 7.4, with NaOH. mIPSCs were recorded in the presence of tetrodotoxin (1 μM) and kynurenic acid (1 mM) to block fast sodium spikes and fast glutamatergic excitatory postsynaptic events, respectively. To gain a better resolution of the kinetic properties of GABA$_A$ receptors, all the electrophysiological experiments have been performed at room temperature (22–24 °C) rather than at physiological temperatures (35 °C). This choice is also justified by the fact that, at higher temperatures, the recordings (particularly in the excised patch mode) are very unstable and therefore not particularly suitable for the kinetic analysis performed in the present experiments. For the analysis requiring a high temporal resolution (*e.g.* rise time kinetics of synaptic and evoked currents) signals were low pass-filtered at 10 kHz with a Butterworth filter and sampled at 50–100 kHz using the analog-to-digital converter CED 1401 (Cambridge Electronic Design, Cambridge, UK) and stored on a computer hard disk. The data and acquisition software were kindly given by Dr. J. Dempster (Strathclyde University, Glasgow, UK).

GABA was applied to excised patches using an ultrafast perfusion system based on a piezoelectric-driven theta glass application pipette (24). The piezoelectric translator was from Physik Instrumente (Waldbronn, Germany), and theta glass tubing was from Hilgenberg (Malsfeld, Germany). The time course of the solution exchange was estimated by liquid junction potential measurements. The application of a 10%-diluted external solution to the open tip patch pipette evoked a junctional current. The establishment of this current represents the complete solution exchange around the patch pipette. The 10–90% of this process occurred in 40–80 μs (10–90% solution exchange time).

The speed of the solution exchange was also estimated around the excised patch by the 10–90% onset of the membrane depolarization induced by application of high (25 mM) potassium saline. In this case the 10–90% rise time value (60–90 μs) was very close to that found for the open tip recordings.

Data Analysis—Miniature synaptic currents were analyzed with the AxoGraph 3.5.5 program (Axon Instruments, Foster City, CA). This program uses a detection algorithm based on a sliding template. The template did not induce any bias in the sampling of events, because it was moved along the data trace one point at a time and was optimally scaled to fit the data at each position. The detection criterion was calculated from the template-scaling factor and from how closely the scaled template fitted the data. The threshold for detection was set at 3.5 times the S.D. of the baseline noise. Using the same program, the decay time constant of averaged mIPSCs was taken from the biexponential fit of the decay time. The rise time was estimated as the time needed for 10–90% increase of the peak current response.

The decaying phase of the mIPSCs and GABA-evoked currents was fitted with exponential functions in the form,

$$y(t) = \sum_{i=1}^{n} A_i * \exp(-t/\tau_i) \qquad \text{(Eq. 1)}$$

where τ_i and A_i are the time constants and relative fractions of the respective components In the case of analysis of normalized currents, the fractions of kinetic components fulfilled the normalization condition, as in Equation 2.

$$\sum_{i=1}^{n} A_i = 1 \qquad \text{(Eq. 2)}$$

Deactivation time courses of mIPSCs and GABA-evoked currents were fitted with a sum of two and three exponentials, respectively ($n = 2$ and $n = 3$).

The mean time constant calculated as,

$$\tau_{mean} = \sum_{i=1}^{n} A_i * \tau_i \qquad \text{(Eq. 3)}$$

was used to estimate the speed of the decaying process. In the case of current responses elicited by long (250 ms) GABA pulses, the desensitization onset was described by,

$$y(t) = A_{fast} * \exp(-t/\tau_{fast}) + A_{slow} * \exp(-t/\tau_{slow}) + A_s \qquad \text{(Eq. 4)}$$

where A_{fast} and A_{slow} are the fractions of the fast and the slow component, respectively, and τ_{fast} and τ_{slow} are the fast and the slow time constants. A_s is the steady state current.

The goodness of the fit was assessed by minimizing the sum of the squared differences. Brief (2 ms) paired pulses separated by a variable time interval were used to test whether or not the entrance of bound receptors into the desensitized state proceeded after the agonist removal. The parameter R was calculated according to the formula,

$$R = (I_2 - I_{end})/(I_1 - I_{end}) \qquad \text{(Eq. 5)}$$

where I_1 is the first peak amplitude, I_{end} is the current value immediately before the application of the second pulse, and I_2 is the second peak amplitude. During the 2-ms pulse the onset of the use-dependent desensitization is minimal. Thus, in the case of continued entrance into

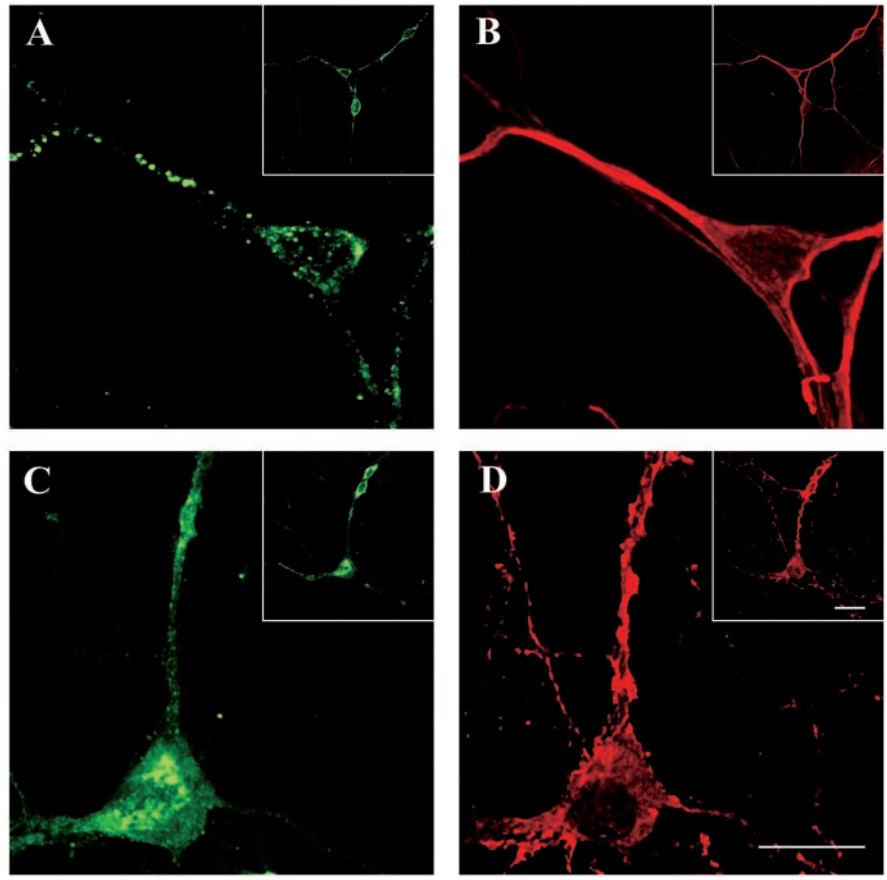

FIG. 1. **Nocodazole treatment promotes GABA$_A$ receptor clusters disassembly.** *A* and *C*, surface staining of GABA$_A$ receptor γ_2 subunit in unpermeabilized control neurons (*A*) and nocodazole-treated (*C*) cells visualized using an affinity-purified rabbit polyclonal antibody followed by fluorescein isothiocyanate-labeled goat anti-rabbit IgG. *B* and *D*, after permeabilization the same cells shown in *A* and *C* were labeled with a rat monoclonal anti-tubulin antibody followed by rhodamine-labeled rabbit anti-rat IgG. Samples were analyzed by confocal microscopy. *Scale bars* = 10 μm. *Insets* in *A–D* show a low magnification of the corresponding fields. *Scale bar* = 20 μm.

the desensitized state after the first short agonist pulse, the peak of the second response (I_2) was smaller than the first one resulting in $R < 1$. Simulation experiments were performed using the Bioq software (kindly provided by Dr. H. Parnas, Hebrew University, Jerusalem). The Bioq software converted the kinetic model (see Fig. 8*A* below) into a set of differential equations and solved them numerically. Because in the absence of agonist receptors can spontaneously open at very low probability (25–27), for simulation convenience it was assumed as the initial condition, *i.e.* at $t = 0$ no bound or open receptors were present. Various experimental protocols were investigated by "clamping" the agonist concentration time course in the form of square-like pulses (ultrafast perfusion experiments). The solution of such equations yielded the time courses of probabilities of all the states assumed in the model. The fit of the experimental data was performed by optimizing the values of rate constants. The procedure for the rate constants optimization was based on the comparison of the time course of recorded currents and that of simulated responses. As described in detail under "Results," specific experimental protocols were used to estimate different sets of rate constants.

Data are expressed as mean ± S.E., and all the values included in the statistics represent recordings from separate cells. Unless otherwise stated, statistical comparisons were made with the use of unpaired *t* test, Wilcoxon signed rank test, and Kolmogorov-Smirnov test ($p < 0.05$ was taken as significant).

RESULTS

Nocodazole Treatment Induces the Depolymerization of Microtubules and the Declusterization of GABA$_A$ Receptors—GABA$_A$ receptor clusterization is known to be dependent on the presence of the intact cytoskeleton. Nocodazole was tested on cultured hippocampal neurons for its ability to depolymerize microtubules and disrupt the cytoskeleton. Neurons were incubated with nocodazole (10 μg/ml) for 20, 40, 60, and 120 min at 37 °C and then immunostained for tubulin. Progressive disruption of microtubules occurred with the increasing duration of the incubation time. By 40 min most of the microtubules were depolymerized (data not shown). Bath application of nocodazole for 2 h at room temperature and 37 °C produced similar microtubule disruption ($n = 4$, data not shown), indicating that incubation temperature does not influence nocodazole effect.

Then the organization of GABA$_A$ receptors in the plasma membrane was analyzed upon nocodazole-induced depolymerization of microtubules. In control conditions, the typical branched microtubule bundles were associated with brightly stained clusters of GABA$_A$ receptors on the soma and dendrites (Fig. 1, *A* and *B*). After nocodazole treatment for 1–2 h, the disassembly of the microtubular network was accompanied by a redistribution of GABA$_A$ receptors, because they were diffusely expressed throughout the surface of the cells or still belonged to residual puncta (Fig. 1, *C* and *D*). These experiments provide evidence that nocodazole is able to depolymerize microtubules and to induce GABA$_A$ receptors declusterization in cultured hippocampal neurons.

Nocodazole Treatment Affects the Onset Kinetics of mIPSCs—mIPSCs were recorded from cultured hippocampal neurons in the whole-cell configuration of the patch-clamp technique at a holding potential of −70 mV in the presence of tetrodotoxin (1 μM) and kyneurenic acid (1 mM). Miniature events were reversibly blocked by bicuculline (10 μM) indicating that they were GABA$_A$-mediated (data not shown). mIPSCs were recorded from untreated neurons (control), and cells were incubated for 2 h with nocodazole (10 μg/ml). Nocodazole treatment induced a significant ($p < 0.0001$) acceleration of the current onset: in control conditions, the mean 10–90% rise time of mIPSCs was 0.96 ± 0.03 ms ($n = 35$), whereas in cells treated with nocodazole it was 0.72 ± 0.02 ms ($n = 29$, Fig. 2*A*). This acceleration resulted in a significant ($p < 0.001$) shift to the left of the cumulative rise time distribution (Fig. 2*B*). Nocodazole treatment did not significantly ($p > 0.05$) affect the mean frequency of mIPSCs (0.67 ± 0.11 and 0.46 ± 0.10 Hz, in control and nocodazole, respectively, data not shown). Although nocodazole

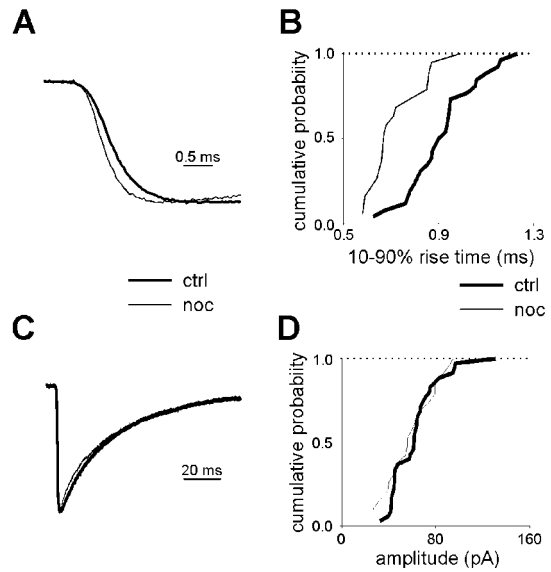

FIG. 2. **Bath treatment with nocodazole accelerates the kinetics of mIPSCs.** *A*, normalized onset of mIPSCs recorded from a control (*thick line*) and nocodazole-treated (*thin line*) neurons. Each *trace* is the average of 55 individual events. *B*, cumulative 10–90% rise time distribution of mIPSCs in control conditions (*thick line*) and after nocodazole treatment (*thin line*). *C*, normalized and superimposed traces of mIPSCs recorded in control (*thick line*) and in nocodazole-treated (*thin line*) neurons. Each *trace* is the average of 55 mIPSCs. *D*, cumulative amplitude distribution of mIPSCs in control and nocodazole (*thick* and *thin lines*, respectively).

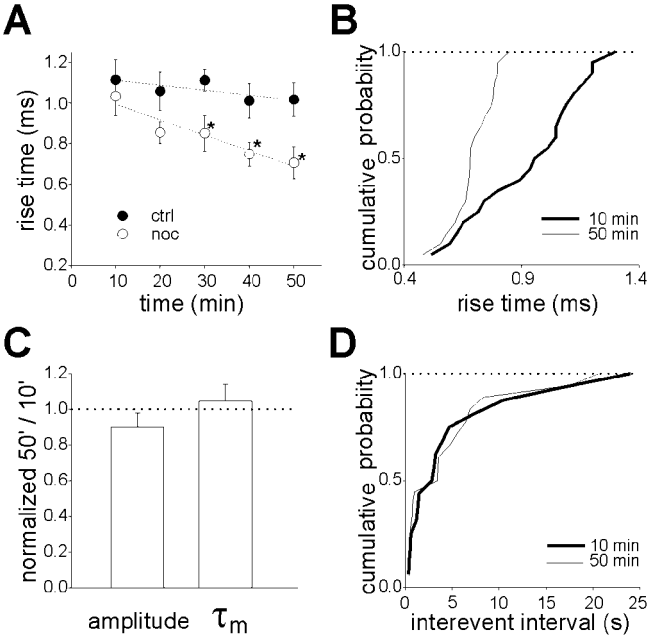

FIG. 3. **Intrapipette application of nocodazole affects the onset kinetics of mIPSCs.** *A*, each data point represents the average 10–90% mean rise time of mIPSCs recorded during 10-min epochs in control conditions (*filled circles*, $n = 10$) and in the presence of nocodazole in the pipette (*open circles*, $n = 11$). *, $p < 0.05$. *B*, cumulative 10–90% rise time distribution of the miniature events recorded during the first 10-min epoch (*thick line*) and the last 10-min epoch (*thin line*) during intrapipette application of nocodazole ($n = 11$). *C*, mean amplitude and averaged τ_{mean} (τ_m) of mIPSCs recorded during the last 10 min, normalized to the corresponding values recorded during the first 10 min ($n = 11$). *D*, cumulative interevent interval distribution of mIPSCs recorded during the first (*thick line*) and the last (*thin line*) 10-min epochs during intrapipette application of nocodazole in 11 neurons.

treatment induced a slight reduction of the mean peak amplitude (from 63.2 ± 3.4 to 58.6 ± 4.8 pA), and this difference was not significant ($p > 0.05$). Moreover, the cumulative amplitude distribution of mIPSCs was not significantly different from control ($p > 0.05$; Fig. 2*D*). The decay of mIPSCs was unaffected by nocodazole: current decay was fitted with a biexponential function with time constants τ_{fast} and τ_{slow} of 8.0 ± 0.7 and 39.7 ± 1.9 ms ($A_{fast} = 0.35$) and 6.3 ± 0.8 and 36.4 ± 3.6 ms ($A_{fast} = 0.33$) in control and in nocodazole treated neurons, respectively (Fig. 2*C*). This resulted in a mean time constant (τ_{mean}) of 28.1 ± 1.2 (control) and 26.1 ± 2.3 ms (nocodazole). Altogether, these results indicate that the declusterization of GABA$_A$ receptors subsequent to microtubule disruption accelerates the onset kinetics of mIPSCs. Moreover, the lack of a clear effect of nocodazole on mIPSCs frequency suggests that this drug does not have a main effect on transmitter release.

To confirm this hypothesis, further experiments were performed by adding nocodazole into the patch pipette, so as to disrupt microtubules only in the recorded cell. Currents were recorded for at least 50 min to allow nocodazole to produce its effect (as detected from immunocytochemical experiments). mIPSCs recorded in 10-min epochs were pooled together and then analyzed. In control conditions ($n = 10$) the onset of mIPSCs did not significantly change with time, and no signs of rundown were observed. During intrapipette application of nocodazole ($n = 11$) a progressive acceleration of mIPSCs onset was observed (Fig. 3*A*). Compared with controls, in the presence of nocodazole a significant ($p < 0.05$) reduction of mIPSCs rise time was detected from 30 min on. The linear regression curves through the data points obtained in control and in the presence of nocodazole had almost the same intercept, indicating that, starting from similar conditions, it took some time for nocodazole to produce its effect. If we considered the first 10 min of intrapipette application of nocodazole as internal control, the progressive reduction of the rise time became significant ($p < 0.05$) after 40 min. The cumulative rise time distribution of the events recorded during the last 10 min was significantly ($p < 0.001$) shifted to the left compared with that relative to the first 10 min (Fig. 3*B*). This result was consistent with the immunocytochemical data showing that it takes less than 40 min for nocodazole to considerably disrupt microtubules and to induce the declusterization of GABA$_A$ receptors.

No significant changes ($p > 0.05$) in the peak amplitude and decay of mIPSCs occurred during intrapipette application of nocodazole. During the first and the last 10-min epochs, the peak amplitude was 58.4 ± 2.7 and 52.5 ± 4.9 pA, respectively, whereas τ_{mean} was 28.2 ± 2.3 and 29.9 ± 4.0 ms, respectively (Fig. 3*C*).

Similarly to the bath treatment, the intrapipette application of nocodazole did not alter the frequency of mIPSCs, because the cumulative interevent interval distributions of mIPSCs recorded at 10 and 50 min were similar ($p > 0.05$, Fig. 3*D*). The lack of changes in mIPSCs frequency obtained after bath treatment and during intrapipette application of nocodazole suggests that the main site of action of this drug is postsynaptic.

Nocodazole Accelerates the Onset Kinetics of Currents Evoked by Ultrafast Applications of GABA—The use of the ultrafast agonist application system allows determination of the microscopic gating of GABA$_A$ receptors with a time resolution adequate to synaptic events (28–30). Firstly we have investigated the possible direct effect of nocodazole on the kinetic properties of GABAergic currents. GABA was applied alone or with nocodazole to the same patch excised from untreated neurons ($n = 6$). The co-application of GABA (10 mM) and nocodazole (10 μg/ml), after a pre-equilibration with nocodazole for 1 min, did not alter the peak amplitude and the kinetic properties of the currents, compared with controls ($p > 0.05$; Fig. 4*A*). In partic-

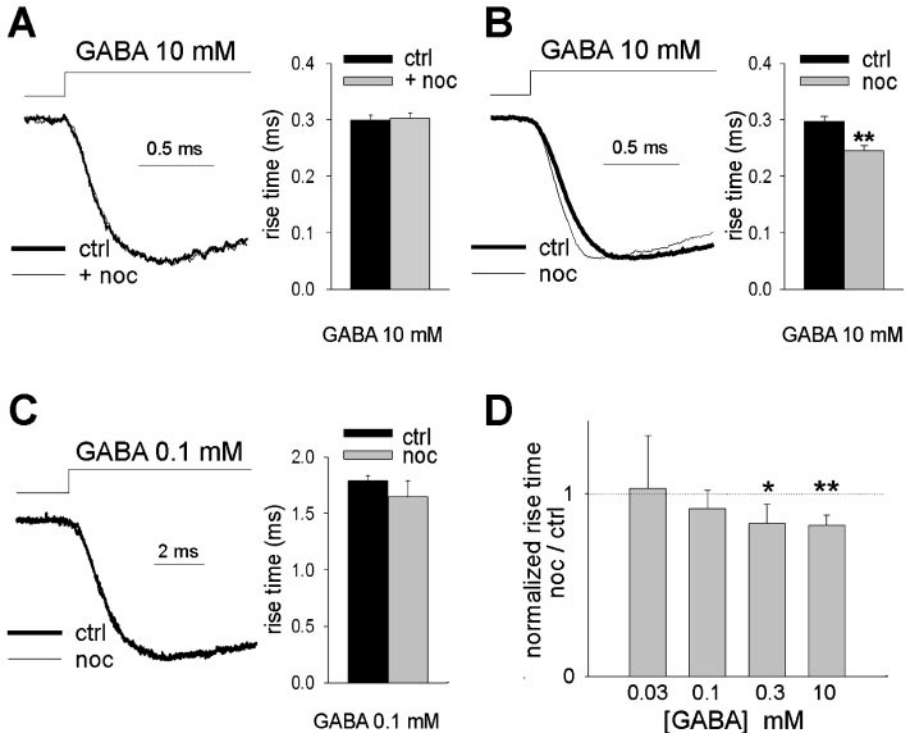

FIG. 4. **Microtubule disruption accelerates the onset of GABA-evoked currents, only at saturating concentration of agonist.** *A* (*left*), normalized and superimposed onset of current responses to 2-ms application of 10 mM GABA (*thick line*) and co-application of 10 mM GABA plus 10 μg/ml nocodazole (*thin line*) after pre-equilibration with nocodazole for 1 min obtained from the same patch. Note that the two traces overlap. *A* (*right*), mean 10–90% rise time of currents evoked by 10 mM GABA in control and by co-application of GABA plus nocodazole on the same patches ($n = 6$). *B* (*left*), normalized and superimposed onset of current responses to 2-ms application of 10 mM GABA from a control (*thick line*) and a nocodazole-treated neuron (*thin line*). Each *trace* is the average of three responses. *B* (*right*), mean 10–90% rise time of currents evoked by 10 mM GABA in control ($n = 26$) and in nocodazole ($n = 29$). *C* (*left*), normalized and superimposed onset of responses to 100 μM GABA in control (*thick line*) and after nocodazole treatment (*thin line*). Each *trace* is the average of four responses. Note that the two traces overlap. *C* (*right*), mean 10–90% rise time of currents evoked by 100 μM GABA in control ($n = 13$) and nocodazole ($n = 15$). *D*, mean 10–90% rise time of currents evoked by different concentrations of GABA in the presence of nocodazole ($n = 7$–29), normalized to the corresponding control values ($n = 8$–26). *, $p < 0.05$; **, $p < 0.01$.

ular, in the absence or presence of this drug, the mean 10–90% rise time and the mean peak amplitude values of GABA-evoked responses were similar (312 ± 25 μs and 375 ± 48 pA in control, *versus* 302 ± 32 μs and 412 ± 74 pA in nocodazole, respectively, $n = 6$, paired t test $p > 0.05$, Fig. 4*A*). Single applications of GABA ($n = 10$) or GABA plus nocodazole ($n = 9$) were also tested in different patches. Again nocodazole (10 μg/ml) did not induce any modification in the shape of GABA-evoked currents. The 10–90% rise time was 309 ± 15 and 314 ± 19 μs and the peak amplitude was 371 ± 78 and 352 ± 89 pA, in control and co-application of nocodazole, respectively ($p > 0.05$). Altogether these data demonstrate that nocodazole does not have a direct effect on GABA$_A$ receptors.

To investigate the mechanisms underlying the changes of mIPSCs kinetics induced by GABA$_A$ receptor declusterization, currents evoked by ultrafast applications of GABA were studied with different protocols in patches excised from nocodazole-treated neurons. Similarly to mIPSCs, nocodazole treatment (10 μg/ml, for 2 h) induced an acceleration of the onset of currents evoked by brief (2 ms) pulses of a saturating concentration of GABA (10 mM, Fig. 4*B*, *left*). In these conditions, the value of the mean 10–90% rise time of GABA-evoked currents was significantly ($p < 0.01$) smaller than control (297 ± 9 and 245 ± 8 μs, in control, $n = 29$, and nocodazole, $n = 26$, respectively, Fig. 4*B*, *right*). According to the kinetic model proposed by Jones and Westbrook (28) (see Fig. 8*A*), the activation of GABA$_A$ receptor is the result of two kinetically separated steps: the binding of the agonist to the receptor and the conformational change from the bound-closed to the bound-open state. It is worth noting, however, that, once the binding step is completed, the receptor may enter either the fully bound open or desensitized state and therefore the rate of entrance into the desensitized state directly affects the occupancy of the open state. Among the steps reported in the model we are referring to, the only one whose kinetics is dependent on GABA concentration is the binding (the effective rate of binding is proportional to $k_{on} \times$ [GABA]). Thus, at low GABA concentrations, the binding step becomes much slower than the conformational change and is thus rate-limiting. In this way the study of macroscopic current onset at low concentrations of GABA sheds light on the binding step. For this reason GABA responses elicited by GABA concentrations ranging between 3 and 300 μM were recorded from control and nocodazole-treated neurons. In this range of agonist concentrations any difference in the onset kinetics could be ascribed to a modification of the binding rate constant. Nocodazole did not affect the onset of current responses evoked by low concentrations of GABA up to 100 μM (Fig. 4, *C* and *D*) but significantly ($p < 0.05$) reduced the mean 10–90% rise time of currents evoked by GABA 300 μM (Fig. 4*D*). A modification in the binding rate after nocodazole treatment would be expected to affect the onset of currents evoked by a broad spectrum of non-saturating GABA concentrations. Moreover, at 300 μM GABA, current onset is close to saturation and it is possible that the nocodazole-induced acceleration of current rising phase results from the modulation of conformational transition rather that from faster binding (at this GABA concentration the binding rate is comparable to that of the conformational change). These data suggest that nocodazole-induced microtubule disruption and GABA receptor declusterization do not influence the binding process and thus the binding rate constant k_{on}.

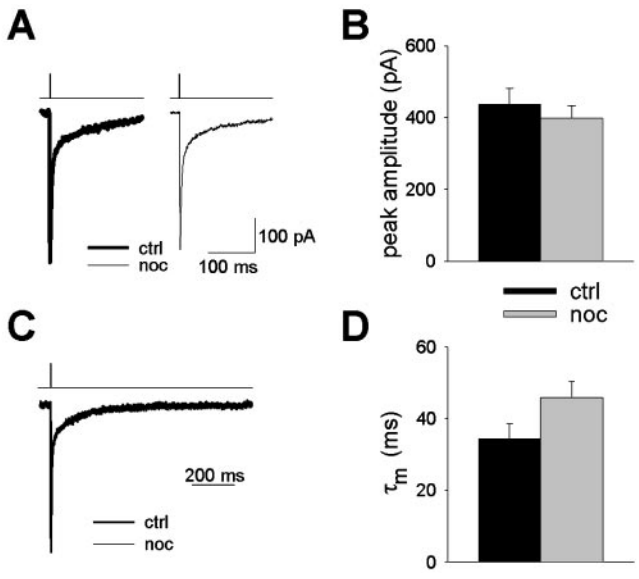

FIG. 5. **Nocodazole treatment does not affect the peak amplitude and the decay of GABA-evoked currents.** *A*, current responses to short (2 ms) pulses of 10 mM GABA (*upper trace*) in control (*thick line*) and nocodazole (*thin line*). *B*, mean peak amplitude of GABA-evoked currents in control conditions and after nocodazole treatment. *C*, normalized and superimposed traces of currents evoked by brief pulses (2 ms) of GABA (10 mM) in control conditions (*thick line*) and after nocodazole treatment (*thin line*). Note that the two traces overlap. *D*, averaged τ_{mean} (τ_m) of GABA-evoked currents in control (n = 12) and in nocodazole (n = 18).

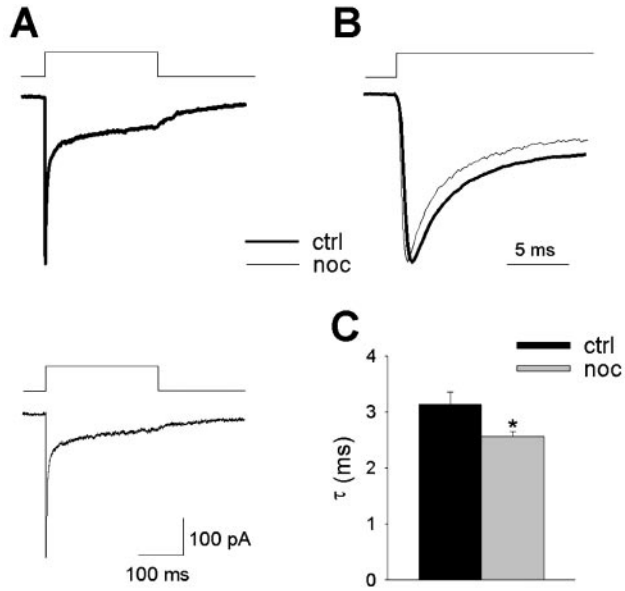

FIG. 6. **Microtubule disruption accelerates the onset of desensitization of GABA-evoked currents.** *A*, currents evoked by long (250 ms) pulses of GABA in control (*thick line*) and nocodazole-treated (*thin line*) neurons. *B*, normalized and superimposed traces of the first 15 ms of currents evoked by long pulses of GABA in control (*thick line*) and after nocodazole (*thin line*) treatment. *C*, mean time constant (τ) of the fitted first 15-ms current responses in control neurons (n = 10) and in nocodazole-treated neurons (n = 11, *, $p < 0.05$). In this time range current desensitization onset was fitted with a monoexponential function.

Effect of Nocodazole on the Peak Amplitude and Decay of GABA-evoked Currents—Short (2 ms) pulses of a saturating concentration of GABA (10 mM) were applied to patches excised from control and nocodazole-treated neurons. A non-statistically significant ($p > 0.05$) reduction of the mean peak amplitude of GABA-evoked currents was observed after microtubule disruption (from 435 ± 45 to 398 ± 34 pA, in control and in nocodazole, respectively; Fig. 5, *A* and *B*). Similarly to mIPSCs, the decay of GABA-evoked currents was not significantly ($p > 0.05$) affected by nocodazole treatment, being the τ_{mean} 34.3 ± 4.3 ms and 45.7 ± 4.4 ms (n = 12–18), in control and nocodazole, respectively (Fig. 5, *C* and *D*).

Nocodazole Accelerates the Desensitization Kinetics of GABA-evoked Currents—It is known that GABA$_A$ receptor rapidly undergoes desensitization during activation. This process is thought to be involved in shaping synaptic currents (28, 31). For this reason an ultrafast agonist application system is necessary to resolve the fast desensitization of GABA$_A$ receptors. To address this issue, a set of experiments was performed applying long pulses (250 ms) of saturating GABA concentration (10 mM). Current desensitization was fitted with biexponential functions with time constants τ_{fast} = 3.8 ± 0.4 ms and τ_{slow} = 67.1 ± 11.0 ms (A_{fast} = 0.64 ± 0.02; $A_{s.s.}$ = 0.18 ± 0.02, n = 9; Fig. 6*A*) and τ_{fast} = 3.3 ± 0.1 ms and τ_{slow} = 63.0 ± 5.9 ms (A_{fast} = 0.63 ± 0.04; $A_{s.s.}$ = 0.13 ± 0.02, n = 8; Fig. 6*A*) in control and nocodazole, respectively. Because the slow component of desensitization is unlikely to influence the shape of synaptic currents, we focused only on the first 15 ms when the fast component is predominant. In this case current desensitization was fitted by a monoexponential function (Fig. 6*B*). Nocodazole treatment produced a significant acceleration of the desensitization onset as the time constant of the fitted current was reduced from 3.12 ± 0.23 ms (A_1 = 0.69 ± 0.02) in control to 2.56 ± 0.09 ms (A_1 = 0.71 ± 0.02) in nocodazole ($p < 0.05$) (Fig. 6*C*).

Nocodazole Treatment Does Not Affect GABA Responses to Paired Pulse Protocols—To analyze the recovery from desensitization, paired pulse protocols are commonly used. Current responses to the second pulse reveal the fraction of receptors able to be activated when the second pulse is applied, and therefore they are influenced by the number of receptors that have recovered from the desensitized state. It should be stressed, however, that the recovery of the second peak reflects not only the recovery from desensitization but a more complex process, including multiple re-entries into the open and desensitized states due to the functional coupling between desensitization-resensitization, opening-closing, and unbinding, and therefore it reveals important information about the proportions between respective rate constants (28, 30, 31).

Paired pulses (2-ms duration each) of saturating GABA (10 mM) were applied at different time intervals ranging between 5 ms and 3 s (Fig. 7*A*). The percentage of recovery of the second peak at each time interval was calculated according to the formula reported under "Experimental Procedures." After microtubule disruption the time course of the recovery of the second peak was not changed with respect to control ($p > 0.05$, Fig. 7*B*).

Model Simulations—The present findings demonstrate that declusterization of GABA$_A$ receptors following microtubule disruption produces similar effects on both mIPSCs and GABA-evoked currents, namely it accelerates the current onset without significantly affecting the current decay or the peak amplitude. Moreover, the experiments using an ultrafast agonist application system provided evidence that nocodazole accelerates the onset of desensitization of GABA-evoked currents without affecting the recovery of the second peak in paired pulses protocols. In the attempt to reconstruct the gating properties of declustered GABA$_A$ receptors, model simulations were used. We referred to the kinetic model proposed by Jones and Westbrook (28) (Fig. 8*A*), which fulfills the minimum requirement to adequately reproduce the gating of GABA$_A$ receptors in different experimental protocols. As shown in the model, all the kinetic states that the receptor may occupy are functionally

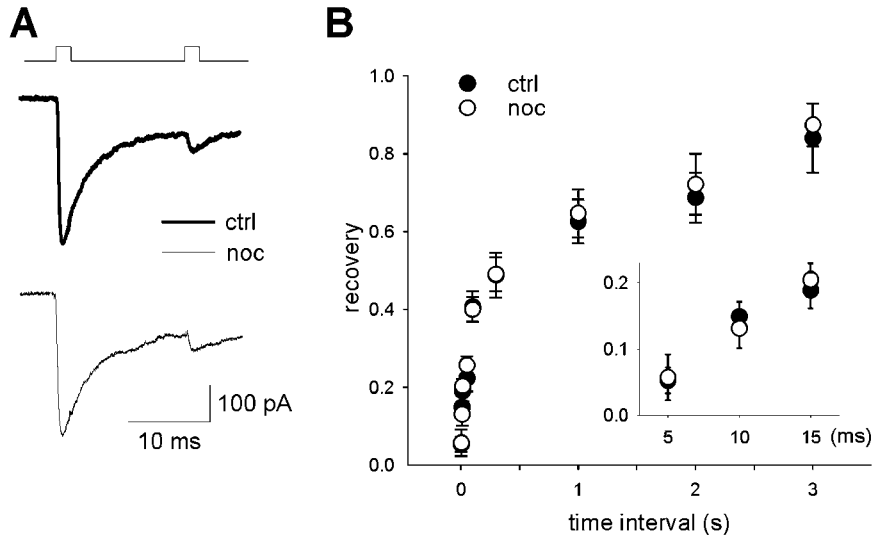

FIG. 7. **Nocodazole treatment does not affect the recovery of the second peak in the paired pulse protocols.** *A*, paired pulses of GABA (2 ms, 10 mM) elicited at a 15-ms interval in control conditions (*thick line*) and after microtubule disruption (*thin line*). *B*, normalized recovery of the second peak evoked in control (*filled circles*) and after nocodazole treatment (*open circles*). Each point represents the mean of five to nine experiments. In the *inset* a part of the plot has been enlarged to show the recovery of the second peak at the shortest time intervals.

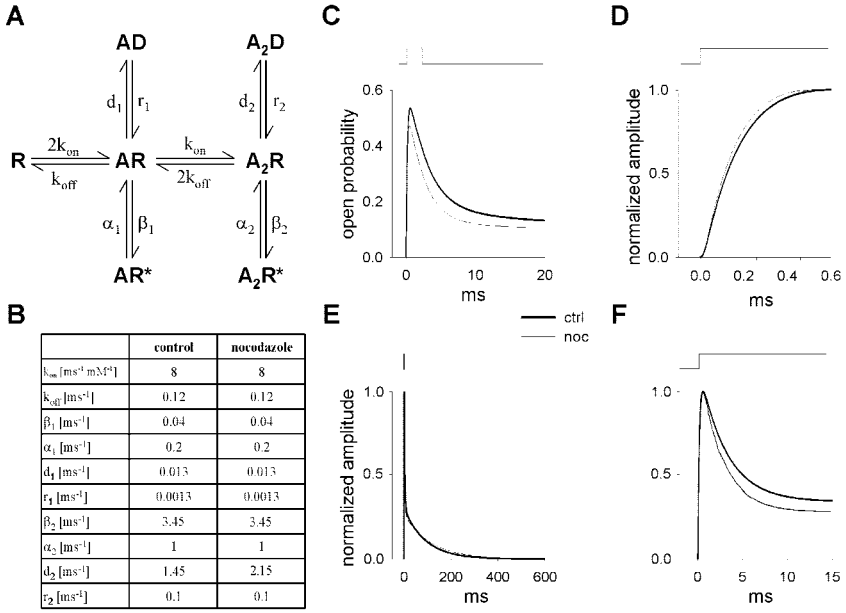

	control	nocodazole
k_{on} [ms^{-1} mM^{-1}]	8	8
k_{off} [ms^{-1}]	0.12	0.12
β_1 [ms^{-1}]	0.04	0.04
α_1 [ms^{-1}]	0.2	0.2
d_1 [ms^{-1}]	0.013	0.013
r_1 [ms^{-1}]	0.0013	0.0013
β_2 [ms^{-1}]	3.45	3.45
α_2 [ms^{-1}]	1	1
d_2 [ms^{-1}]	1.45	2.15
r_2 [ms^{-1}]	0.1	0.1

FIG. 8. **Model simulations of the effect of nocodazole treatment on the kinetics of GABA-evoked currents.** *A*, kinetic model proposed by Jones and Westbrook (28). According to their model, the receptor (*R*) binds in sequence two molecules of agonist (*A*), reaching the doubly bound and closed state (A_2R). From this state it can open or desensitize (A_2R^* or A_2D, respectively). The singly bound open and desensitized states are also present (AR^* and AD, respectively). *B*, values of the rate constants producing the simulated current responses in control and nocodazole. The values of rate constants of the singly bound states were adopted by Jones and Westbrook (28) and were assumed not to be affected. *C*, simulations of current responses to brief (2 ms, *upper line*) pulses of GABA (10 mM) in control conditions (*thick line*) and in nocodazole (*thin line*). *D* and *E*, normalized onset (*D*) and decay (*E*) of simulated responses to brief pulses (2 ms, *upper line*) of GABA (10 mM) in control (*thick line*) and in nocodazole (*thin line*). *F*, normalized simulation of responses to long pulses (250 ms, *upper line*) of GABA (10 mM) in control (*thick line*) and in nocodazole (*thin line*). Only the first 15 ms are represented.

coupled with the others, and thus current responses are inevitably influenced by all the rate constants that govern the transition from one state to the other (27, 31, 32). However, particular rate constants can be estimated by analyzing current responses obtained in different experimental conditions. Two sets of rate constants that could well reproduce experimental data both in control and after microtubule disruption were chosen. The value of k_{on} was estimated from the current onset kinetics at low GABA concentrations when the binding is the rate-limiting step. The values of the rate constants governing the entry and the exit from the desensitized state (d_2 and r_2, respectively) were evaluated from the time course of currents evoked by long agonist application and paired pulse protocols. The value of the close-to-open rate constant (β_2) and d_2 were adjusted according to the current onset at saturating concentrations of agonist. The open to close rate constant (α_2) and the unbinding rate constant (k_{off}) were optimized to reproduce the decay of currents elicited by 2-ms pulses of saturating concentration of GABA and paired pulse protocols. The rate constants governing the transitions of singly bound states were adopted from Jones and Westbrook (28). It should be noticed, however, that at agonist concentrations of >30 μM the probability of occupancy of singly bound receptors is negligible. Once a complete set of rate constants is found to properly reproduce the experimental data obtained from all the protocols in control conditions, the effect of microtubule disruption on GABA-evoked currents was included in the simulations.

Surprisingly, increasing the value of d_2 was sufficient to reliably simulate the experimental current responses to different protocols (Fig. 8*B*). The increase in d_2 may account for the accelerated onset of desensitization (Fig. 8*F*). Moreover, according to the basic properties of bifurcating reactions, the increase

in d_2 may result in a faster current onset (Fig. 8*D*). In fact, the rate of entry into the doubly bound open state at saturating [GABA] can be approximated as $\beta_2 + d_2$ (assuming $\beta_2 \gg \alpha_2$ and $d_2 \gg r_2$), and therefore an increase in d_2 would be expected to accelerate the current onset rate. Indeed also an increase of β_2 (leaving d_2 unchanged) could reproduce the accelerated current onset, but, contrary to our observations, this would have led to an increased peak amplitude. It should be noticed, however, that good resolution could also be obtained by properly increasing the values of both β_2 and d_2, but this set of parameters was excluded as it resulted in a faster recovery of the second peak in the paired pulse protocols. In our simulations the increase in d_2 led to a reduced occupancy of the open state that resulted in a 10% reduction in the peak amplitude of the simulated current. This effect, although present as a trend in our experimental data, was below the significance threshold due to the large variability of the current peak amplitude (Fig. 8*C*). Any change in the resensitization rate constant (r_2) did not produce any significant improvement in the steady state of desensitizing currents (Fig. 8*F*) or in the recovery of the second peak in the paired pulse simulations (data not shown), so this parameter was kept unchanged. The lack of effects of nocodazole on the rising phase of currents evoked by non-saturating [GABA] indicates that the binding rate (k_{on}) is not affected, hence this parameter was not modified in our model. The value of k_{off} was kept unchanged as the current deactivation was unaffected after nocodazole treatment (Fig. 8*E*). Although the deactivation process is known to be shaped by GABA$_A$ receptor desensitization, in our simulations, it was not relevantly affected by the proposed increase of d_2 after nocodazole treatment.

DISCUSSION

The present experiments clearly demonstrate that, in cultured hippocampal neurons, nocodazole-induced declusterization of GABA$_A$ receptors is associated with an acceleration of the onset kinetics of mIPSCs. The quantitative analysis of current responses to ultrafast applications of GABA and model simulations suggest that this effect results from changes in the microscopic gating of GABA$_A$ receptors and in particular from an accelerated entry into the desensitized state.

It is known that the clusterization of native and recombinant GABA$_A$ receptors depends on the presence of the intact cytoskeleton, because microtubule disruption alters the punctuate expression of GABA$_A$ receptors on the plasma membrane (18–20). Among the drugs used to disrupt the cytoskeleton, nocodazole and colchicine are the most frequently employed (12, 33, 34). Because colchicine has been shown to competitively interact with GABA$_A$ receptor binding site (22, 35), we have used nocodazole. Acute application of nocodazole showed that it does not directly interfere with GABA$_A$ receptor function. In agreement with other studies (18, 19) nocodazole treatment considerably altered the organization of GABA$_A$ receptors clusters at the plasma membrane by breaking down the microtubules. GABA$_A$ receptor clusterization has been mainly addressed under a molecular point of view in the attempt to identify the proteins involved in the anchoring and clustering (4, 13, 16, 36–40). However, an accurate analysis of the effect of receptor clusterization on GABAergic transmission has been often neglected, and therefore the present study has focused mainly on the gating properties of diffuse receptors. In a previous study it has been reported that, in declustered recombinant receptors, GABA-evoked currents showed a slower deactivation and a faster desensitization (19), compared with clustered ones. However, as pointed out by the authors, the limited time resolution of the agonist application system precluded the assessment of the kinetic changes occurring at the submillisecond time scale.

A novel and unexpected finding of the experiments reported here was a nocodazole-induced acceleration of the onset kinetics of mIPSC in the absence of any significant effect on the peak amplitude and decay kinetics. These results were related to receptor declusterization following microtubule disruption. However, the widespread effect of nocodazole raises the possibility that this drug affects other targets that in turn may influence GABAergic currents. In fact it has been recently demonstrated that GABA$_A$ receptors clusterization can be regulated in an activity-dependent manner (41, 42). Thus, there is the possibility that bath incubation with nocodazole may increase receptor declusterization by reducing the incoming inputs from presynaptic nerve terminals. However, this possibility is unlikely, because nocodazole treatment did not significantly modify the frequency of spontaneous miniature events. Moreover, the observation that the same results could be achieved when nocodazole was applied into the pipette or in the bath argues against a presynaptic site of action of the drug.

As already mentioned, the analysis of the current evoked in excised patches by ultrafast application of GABA allows to dissect out the kinetic properties of GABA$_A$ receptors under non-equilibrium conditions such as those occurring at the synapse (29, 30). It should be stressed that upon patch excision the detached portion of the membrane is no longer interacting with the intracellular structural and functional proteins and/or intracellular factors. However, the evidence that despite patch excision nocodazole treatment was still able to affect the kinetic properties of GABA-evoked currents suggests that this procedure did not alter GABA$_A$ receptors clusterization. Moreover, the observation that GABA-evoked currents and mIPSCs exhibited similar kinetic changes after nocodazole treatment indicates also that extrasynaptic receptors are clustered in control conditions (40).

Similarly to mIPSCs, currents evoked by saturating concentrations of GABA exhibited a faster onset when elicited from declustered GABA$_A$ receptors. The analysis of the current onset at different agonist concentrations is very useful to distinguish the binding of the agonist (k_{on}) from the conformational change from the doubly bound closed state to the open state (β_2). As already mentioned, the only step in the activation kinetics of GABA$_A$ receptors that is concentration-dependent (28) is the binding of the agonist to the receptor (k_{on}). The lack of changes in the rise time at low agonist concentrations suggests that k_{on} is not altered in declustered receptors. This hypothesis is not in contrast with the accelerated onset of currents evoked by higher concentrations of GABA (starting form 300 μM) when microtubules are disrupted. In those cases in fact the concentration of GABA makes the binding occur faster than the transitions to the open and desensitized states, and so the current onset would reflect the kinetics of the slower steps. According to the Jones and Westbrook model (28), the open and the desensitized states are arranged in a bifurcating reaction and thus, if the values of β_2 and d_2 were comparable, during the activation of GABA$_A$ receptors, the two processes would occur at the same time. For this reason currents have to be analyzed under non-equilibrium conditions, because the recovery from the open and the desensitized states may influence the gating of GABA$_A$ receptors. In line with the basic properties of bifurcating reactions, the onset rate of the two processes should be $\beta_2 + \alpha_2 + d_2 + r_2$. However, being $\beta_2 \gg \alpha_2$ and $d_2 \gg r_2$, the values of α_2 and r_2 can be neglected. For this reason the onset rate of both the open and the desensitized states can be approximately defined as $\beta_2 + d_2$. The nocodazole-induced acceleration of the current onset at high GABA concentrations suggests the increase of at least one of these rate constants. However, model simulations argue against enhancement of β_2,

because it would lead to an increase in current amplitude in contrast with the unchanged amplitude of currents recorded after nocodazole treatment. Although α_2 may play an important role in shaping GABAergic currents, in the present experiments its contribution was not crucial, because an increase in its value did not significantly improve the fit of experimental data. An increased value of d_2, as suggested by the accelerated desensitization onset, may account for the accelerated current onset. The increase of d_2 also led to a 10% reduction of the peak amplitude of the simulated current. In fact, during receptor activation, the entry into the open and desensitized states proceeds together. Thus an increased rate of entry into the desensitized state produces a lower occupancy of the open state leading to a reduction of the open peak probability. However, our experimental data did not show any significant difference in the mean peak amplitude of GABA-mediated currents after nocodazole treatment, possibly due to the large responses variability. Hence, we propose that after nocodazole treatment the promoted entry of declustered $GABA_A$ receptors into the desensitized state reduces the number of "ready to open" receptors and accelerates their onset kinetics. The lack of effect on the decay and on the recovery of the second peak in the paired pulse protocols suggests that nocodazole treatment does not alter the unbinding process (k_{off}). This hypothesis is in line with the "two arms binding site" theory (28, 43, 44), which states that k_{on} and k_{off} are inversely correlated. Thus, the unchanged value of k_{on} could be reasonably associated with an unchanged value of k_{off}, suggesting that the declusterization does not affect the affinity (k_{off}/k_{on}) of $GABA_A$ receptors.

CONCLUSIONS

In the present report we demonstrate that the cytoskeleton is essential for promoting and maintaining $GABA_A$ receptor clusterization and this contributes to the modulation of the GABAergic currents in cultured hippocampal neurons. Differently from previous studies (17, 19) we investigated declustered native $GABA_A$ receptor function under more physiological conditions by analyzing mIPSCs and GABA-evoked currents in cultured hippocampal neurons.

From experimental data and model simulations we propose that the faster current onset may result from an accelerated entrance into the fully bound desensitized state of declustered $GABA_A$ receptors. Our results are in line with the progressively more accepted idea that receptor desensitized state plays a crucial role in shaping synaptic currents (28, 31) and tonic inhibition (45–48).

Acknowledgments—We thank Prof. W. Sieghart for the kind gift of $GABA_A$ receptor γ_2 subunit antibody and M. Righi for his technical support in cell culture. The Bioq software was kindly provided by Dr. H. Parnas from Hebrew University, Jerusalem.

REFERENCES

1. Moss, S. J., and Smart, T. G. (2001) *Nat. Rev. Neurosci.* **2,** 240–250
2. Barnes, E. M., Jr. (2000) *Life Sci.* **66,** 1063–1070
3. Kneussel, M. (2002) *Brain Res. Brain Res. Rev.* **39,** 74–83
4. Wang, H., Bedford, F. K., Brandon, N. J., Moss, S. J., and Olsen, R. W. (1999) *Nature* **397,** 69–72
5. Wang, H., and Olsen, R. W. (2000) *J. Neurochem.* **75,** 644–655
6. Rothman, J. E. (1994) *Nature* **372,** 55–63
7. Sagiv, Y., Legesse-Miller, A., Porat, A., and Elazar, Z. (2000) *EMBO J.* **19,** 1494–1504
8. Kirisako, T., Baba, M., Ishihara, N., Miyazawa, K., Ohsumi, M., Yoshimori, T., Noda, T., and Ohsumi, Y. (1999) *J. Cell Biol.* **147,** 435–446
9. Lang, T., Schaeffeler, E., Bernreuther, D., Bredschneider, M., Wolf, D. H., and Thumm, M. (1998) *EMBO J.* **17,** 3597–3607
10. Garner, C. C., Garner, A., Huber, G., Kozak, C., and Matus, A. (1990) *J. Neurochem.* **55,** 146–154
11. Prior, P., Schmitt, B., Grenningloh, G., Pribilla, I., Multhaup, G., Beyreuther, K., Maulet, Y., Werner, P., Langosch, D., and Kirsch, J. (1992) *Neuron* **8,** 1161–1170
12. Kirsch, J., and Betz, H. (1995) *J. Neurosci.* **15,** 4148–4156
13. Essrich, C., Lorez, M., Benson, J. A., Fritschy, J. M., and Luscher, B. (1998) *Nat. Neurosci.* **1,** 563–571
14. Kneussel, M., Brandstatter, J. H., Laube, B., Stahl, S., Muller, U., and Betz, H. (1999) *J. Neurosci.* **19,** 9289–9297
15. Sassoe-Pognetto, M., Kirsch, J., Grunert, U., Greferath, U., Fritschy, J. M., Mohler, H., Betz, H., and Wassle, H. (1995) *J. Comp. Neurol.* **357,** 1–14
16. Kannenberg, K., Sieghart, W., and Reuter, H. (1999) *Eur. J. Neurosci.* **11,** 1256–1264
17. Whatley, V. J., Mihic, S. J., Allan, A. M., McQuilkin, S. J., and Harris, R. A. (1994) *J. Biol. Chem.* **269,** 19546–19552
18. Meyer, D. K., Olenik, C., Hofmann, F., Barth, H., Leemhuis, J., Brunig, I., Aktories, K., and Norenberg, W. (2000) *J. Neurosci.* **20,** 6743–6751
19. Chen, L., Wang, H., Vicini, S., and Olsen, R. W. (2000) *Proc. Natl. Acad. Sci. U. S. A.* **97,** 11557–11562
20. Ho, W. H., Wang, S. M., and Yin, H. S. (2001) *J. Cell. Biochem.* **83,** 291–303
21. Andjus, P. R., Stevic-Marinkovic, Z., and Cherubini, E. (1997) *J. Physiol.* **504,** 103–112
22. Bueno, O. F., and Leidenheimer, N. J. (1998) *Neuropharmacology* **37,** 383–390
23. van Zundert, B., Alvarez, F. J., Yevenes, G. E., Carcamo, J. G., Vera, J. C., and Aguayo, L. G. (2002) *J. Neurophysiol.* **87,** 640–644
24. Jonas, P. (1995) in *Single-Channel Recording* (Sakmann, B., and Neher, E., eds) pp. 231–243, Plenum, New York
25. Birnir, B., Everitt, A. B., Lim, M. S., and Gage, P. W. (2000) *J. Membr. Biol.* **174,** 21–29
26. Birnir, B., Eghbali, M., Cox, G. B., and Gage, P. W. (2001) *J. Membr. Biol.* **181,** 171–183
27. Bianchi, M. T., and Macdonald, R. L. (2001) *J. Neurosci.* **21,** 9083–9091
28. Jones, M. V., and Westbrook, G. L. (1995) *Neuron* **15,** 181–191
29. Mozrzymas, J. W., Barberis, A., Michalak, K., and Cherubini, E. (1999) *J. Neurosci.* **19,** 2474–2488
30. Barberis, A., Cherubini, E., and Mozrzymas, J. W. (2000) *J. Neurosci.* **20,** 8618–8627
31. Mozrzymas, J. W., Barberis, A., Mercik, K., and Zarnowska, E. D. (2003) *J. Neurophysiol.* **89,** 871–883
32. Colquhoun, D. (1998) *Br. J. Pharmacol.* **125,** 924–947
33. Baas, P. W., Slaughter, T., Brown, A., and Black, M. M. (1991) *J. Neurosci. Res.* **30,** 134–153
34. Ligon, L. A., and Steward, O. (2000) *J. Comp. Neurol.* **427,** 351–361
35. Weiner, J. L., Buhler, A. V., Whatley, V. J., Harris, R. A., and Dunwiddie, T. V. (1998) *J. Pharmacol. Exp. Ther.* **284,** 95–102
36. Craig, A. M., Blackstone, C. D., Huganir, R. L., and Banker, G. (1994) *Proc. Natl. Acad. Sci. U. S. A.* **91,** 12373–12377
37. Koulen, P., Sassoe-Pognetto, M., Grunert, U., and Wassle, H. (1996) *J. Neurosci.* **16,** 2127–2140
38. Scotti, A. L., and Reuter, H. (2001) *Proc. Natl. Acad. Sci. U. S. A.* **98,** 3489–3494
39. Beck, M., Brickley, K., Wilkinson, H. L., Sharma, S., Smith, M., Chazot, P. L., Pollard, S., and Stephenson, F. A. (2002) *J. Biol. Chem.* **277,** 30079–30090
40. Christie, S. B., Li, R. W., Miralles, C. P., Riquelme, R., Yang, B. Y., Charych, E., Wendou, Y., Daniels, S. B., Cantino, M. E., and De Blas, A. L. (2002) *Prog. Brain Res.* **136,** 157–180
41. Christie, S. B., Miralles, C. P., and De Blas, A. L. (2002) *J. Neurosci.* **22,** 684–697
42. Kilman, V., van Rossum, M. C., and Turrigiano, G. G. (2002) *J. Neurosci.* **22,** 1328–1337
43. Jones, M. V., Sahara, Y., Dzubay, J. A., and Westbrook, G. L. (1998) *J. Neurosci.* **18,** 8590–8604
44. Jones, M. V., Jonas, P., Sahara, Y., and Westbrook, G. L. (2001) *Biophys. J.* **81,** 2660–2670
45. Overstreet, L. S., Jones, M. V., and Westbrook, G. L. (2000) *J. Neurosci.* **20,** 7914–7921
46. Bianchi, M. T., Haas, K. F., and Macdonald, R. L. (2002) *Neuropharmacology* **43,** 492–502
47. Legendre, P., Muller, E., Badiu, C. I., Meier, J., Vannier, C., and Triller, A. (2002) *Mol. Pharmacol.* **62,** 817–827
48. Yeung, J. Y., Canning, K. J., Zhu, G., Pennefather, P., MacDonald, J. F., and Orser, B. A. (2003) *Mol. Pharmacol.* **63,** 2–8

Declusterization of $GABA_A$ Receptors Affects the Kinetic Properties of GABAergic Currents in Cultured Hippocampal Neurons

Enrica Maria Petrini, Paola Zacchi, Andrea Barberis, Jerzy W. Mozrzymas and Enrico Cherubini

J. Biol. Chem. 2003, 278:16271-16279.
doi: 10.1074/jbc.M213081200 originally published online February 24, 2003
